J Electroceram (2012) 28:165–171
DOI 10.1007/s10832-012-9700-0

High temperature electronic properties of $BaTiO_3$ – $Bi(Zn_{1/2}Ti_{1/2})O_3$ – $BiInO_3$ for capacitor applications

Natthaphon Raengthon · David P. Cann

Received: 19 December 2011 / Accepted: 24 February 2012 / Published online: 11 March 2012

Abstract Solid solutions $xBaTiO_3 – (1\text{-}x)(0.5Bi(Zn_{1/2}Ti_{1/2})O_3 – 0.5BiInO_3)$, where x=0.95–0.60, were prepared by conventional mixed oxide method. The single phase perovskite structure was obtained for the composition with x≥ 0.75. Phase transformation from tetragonal to pseudocubic was observed from x-ray diffraction patterns when x decreased from 0.95 to 0.75. In tetragonal phase region, x≥0.90, the increase of $Bi(Zn_{1/2}Ti_{1/2})O_3$ – $BiInO_3$ content decreased the tetragonality and the temperature at which the relative permittivity is maximum (T_{max}). The increase in lattice parameter and T_{max} were observed in the pseudocubic phase region, x<0.90. Additionally, a highly broad and diffuse phase transition was observed from the dielectric data in the pseudocubic phase region. The introduction of Ba vacancies in compositions with x=0.80 and 0.75 also improved dielectric loss at high temperatures. The incorporation of $BiInO_3$ into the $BaTiO_3$ – $Bi(Zn_{1/2}Ti_{1/2})O_3$ compound was also found to improve the temperature coefficient of the relative permittivity, with values as low as approximately −1,000 ppm/K. Overall, ternary perovskite solid solutions based on adding $Bi(Zn_{1/2}Ti_{1/2})O_3$ – $BiInO_3$ to $BaTiO_3$ shows excellent potential for high temperature capacitor applications

Keywords High temperature capacitor · Bi-based perovskite · $BiInO_3$ · $Bi(Zn_{1/2}Ti_{1/2})O_3$ · $BaTiO_3$ · Insulation resistance

N. Raengthon (✉) · D. P. Cann
Materials Science, School of Mechanical, Industrial, and Manufacturing Engineering, Oregon State University, Corvallis, OR 97330, USA
e-mail: natthaphonr@gmail.com

1 Introduction

Perovskite materials possess excellent and unique properties such as piezoelectricity and ferroelectricity. They have been utilized in many applications such as sensors, transducers, ferroelectric random access memories (FRAM), capacitors, and many others [1]. A wide variety of perovskite solid solutions have been developed over years for such applications. The excellent performance of Bi-perovskites in solid solution with Pb-based perovskites were predicted and reported [2, 3]. For example, $PbTiO_3$ – $Bi(Zn_{1/2}Ti_{1/2})O_3$ [4–6], $PbTiO_3$ – $Bi(Mg_{1/2}Ti_{1/2})O_3$ [7, 8], $PbTiO_3$ – $Bi(Ni_{1/2}Ti_{1/2})O_3$ [9], $PbTiO_3$ – $BiScO_3$ [10, 11], and $PbTiO_3$ – $BiInO_3$ [12, 13] compounds have been reported to exhibit a high Curie temperature (T_C), which is a great advantage for high temperature applications. These Bi-perovskites were also investigated in solid solutions with Pb-free ferroelectric materials such as $BaTiO_3$. The $BaTiO_3$ – $BiScO_3$ solid solution exhibited unique properties such as a high energy density due to the existence of weakly-coupled polar nano regions [14]. The $BaTiO_3$ – $Bi(Zn_{1/2}Ti_{1/2})O_3$ solid solutions also shows promising characteristics for high energy density capacitor applications and high temperature capacitor applications [15–17]. Moreover, $BaTiO_3$ – $BiInO_3$ solid solutions have been studied by Datta et al.; however, only a detailed structural analysis was reported [18]. Often, solid solutions of ternary compounds exhibit an improved performance compared to binary compounds, for example, $BaTiO_3$ – $(Bi_{1/2}Na_{1/2})TiO_3$ – $(K_{1/2}Na_{1/2})NbO_3$ [19], $(Bi_{1/2}Na_{1/2})TiO_3$ – $(Bi_{1/2}K_{1/2})TiO_3$ – $Bi((Ni/Mg)_{1/2}Ti_{1/2})O_3$ [20], $BiScO_3$ – $BaTiO_3$ – $(Bi_{1/2}K_{1/2})TiO_3$ [21], and $BaTiO_3$ – $Bi(Zn_{1/2}Ti_{1/2})O_3$ – $BiScO_3$ [22].

The objective of this work is to improve upon the excellent high temperature dielectric properties of $BaTiO_3$ – $Bi(Zn_{1/2}Ti_{1/2})O_3$ ceramics through the addition of $BiInO_3$.

While $BaTiO_3 - Bi(Zn_{1/2}Ti_{1/2})O_3$ has been shown to have a large relative permittivity, low dielectric loss, and excellent insulation resistance, however the temperature coefficient of the relative permittivity (TCε) is greater than −2000 ppm/°C. To address this deficiency, the ternary solid solution based on $BaTiO_3 - Bi(Zn_{1/2}Ti_{1/2})O_3 - BiInO_3$ was investigated in term of structure, dielectric and ferroelectric properties.

2 Experimental procedures

The compound $xBaTiO_3 - (1\text{-}x)(0.5Bi(Zn_{1/2}Ti_{1/2})O_3 - 0.5BiInO_3)$, where x=0.95−0.60, were prepared by using a conventional mixed oxide technique. Metal oxides and carbonates of Bi_2O_3 (>99.9 %), TiO_2 (>99.0 %), ZnO (>99.9 %), In_2O_3 (>99.9 %), and $BaCO_3$ (>99.8 %) were used as starting powders. The powders were mixed and ground in ethanol medium and yttrium-stabilized zirconia milling media by using a vibratory milling machine for six hours and, subsequently, dried in an oven over night. The non-stoichiometric compositions which included 2 mol% of Ba vacancies were synthesized by adjusting the amount of $BaCO_3$ in the batch composition. In order to obtain perovskite phase, the dried powders were first calcined at 800 °C for four hours and then calcined at 950–1100 °C for twelve hours with additional milling step before and after the second calcination step. The calcined powders were mixed with an adequate amount of polyvinyl butyral (PVB) as a binder before forming the ceramic. The green body ceramic discs were prepared by using a uniaxial cold pressing method. The ceramic discs were obtained after sintering at 1100–1280 °C for six hours in air atmosphere by placing the green body in sacrifice powder in alumina crucible with a cover. Silver electrode was put on the ceramic discs by painting the silver paste on parallel specimen with smooth surface, then, fired at 700 °C for 15 min. Perovskite phase formation was confirmed by using an x-ray diffraction technique. The specimen was place in a high temperature measurement cell (NorECS Probostat) for dielectric properties measurement by using an Agilent 4284A LCR meter. A ferroelectric hysteresis loop was investigated at room temperature by using a standard ferroelectrics test system (Radiant Technologies). A measurement of strain as a function of electric field was carried out by using an optical displacement sensor (MTI-2100). To study the insulation resistance, DC resistivity measurements were carried out at different temperatures using a Keithley 237 high voltage source measurement unit. Samples were equilibrated at the measurement temperature for an hour before initiating the measurement.

3 Results and discussion

All of the compositions based on $xBaTiO_3 - (1\text{-}x)(0.5Bi(Zn_{1/2}Ti_{1/2})O_3 - 0.5BiInO_3)$ were sintered to a high density (ρ>95 % $\rho_{Theoretical}$). Diffraction data confirmed that the perovskite structure was obtained by the conventional mixed oxide method. A single phase of perovskite was observed for compositions with x≥0.75. At lower concentration of $BaTiO_3$ (x=0.70 and 0.60), secondary phases, including $Bi_{20}TiO_{32}$, $Bi_4Ti_3O_{12}$, and In_2O_3, were observed in the XRD data, as shown in Fig. 1. The compositions with x=0.95 and 0.90 exhibited tetragonal symmetry, as can be seen by {002} peak splitting and peak distortion. As the concentration of $BaTiO_3$ decreased further (for x=0.85, 0.80 and 0.75), the compounds transformed to pseudocubic symmetry. Regardless of the presence of secondary phases, cubic symmetry was observed for the compositions with x=0.70 and 0.60.

Lattice parameters calculated from the XRD data are shown in Fig. 2. It can be seen that the lattice parameter c decreased for compositions with x=0.95 to x=0.90. Over this same range the lattice parameter a increased. This had the effect of a gradual decrease in the c/a ratio, calculated from the {200} reflections, from 1.011 to 1.005 as the tetragonal phase transitioned to the pseudocubic phase. For compositions with x<0.90, where pseudocubic symmetry was observed, the lattice parameter increased linearly as the concentration of $BaTiO_3$ decreased down to 70 mol%. For x <70 %, where secondary phases were observed, the lattice parameter remained nearly constant. In the literature, for

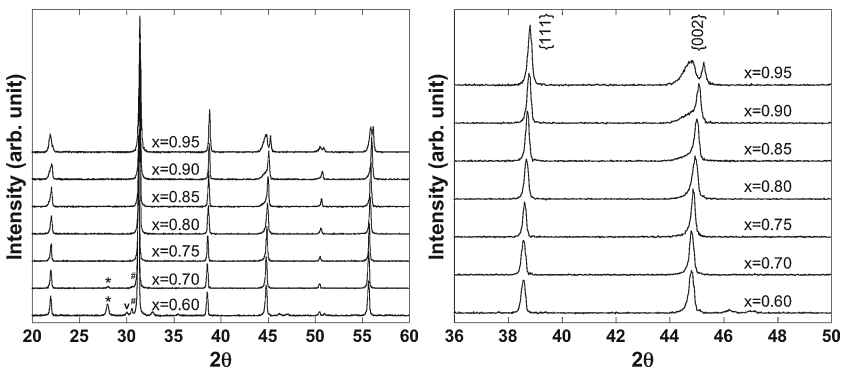

Fig. 1 X-ray diffraction patterns of $xBaTiO_3 - (1\text{-}x)(0.5Bi(Zn_{1/2}Ti_{1/2})O_3 - 0.5BiInO_3)$ ceramics where x=0.95−0.60. The secondary phases including * $Bi_{20}TiO_{32}$, v $Bi_4Ti_3O_{12}$, and # In_2O_3 were observed in the compositions containing less than 75 mol% of $BaTiO_3$

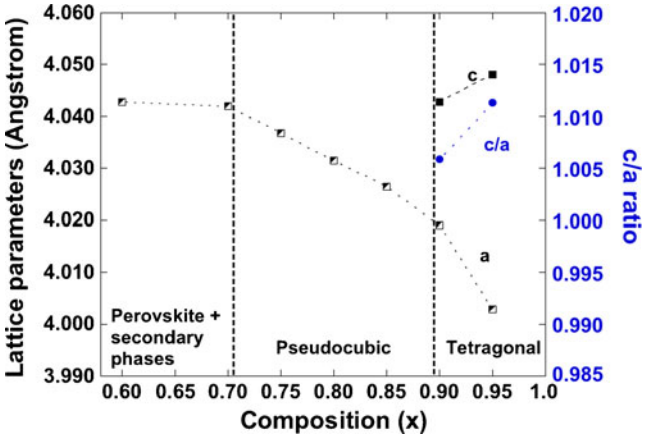

Fig. 2 Lattice parameters and c/a ratio as a function of composition (x) of solid solutions $xBaTiO_3 - (1\text{-}x)(0.5Bi(Zn_{1/2}Ti_{1/2})O_3 - 0.5BiInO_3)$ ceramics where x=0.95−0.75

$BaTiO_3$-based solid solutions it has been shown that the addition of $BiInO_3$ resulted in an increase in the lattice parameter [18] whereas the addition of $Bi(Zn_{1/2}Ti_{1/2})O_3$ resulted in a decrease in the lattice parameter [15]. Therefore, the incorporation of In^{3+}, which is the largest cation on the B-site with a size of 0.8 Å is considerably larger than that of Zn^{2+} (0.740 Å) and Ti^{4+} (0.605 Å), is responsible for the increase of lattice parameter as the concentration of the $Bi(Zn_{1/2}Ti_{1/2})O_3 - BiInO_3$ increased.

As the concentration of the $Bi(Zn_{1/2}Ti_{1/2})O_3 - BiInO_3$ reached 30 mol%, the presence of secondary phases and the constant lattice parameter suggests a solubility limit for $Bi(Zn_{1/2}Ti_{1/2})O_3 - BiInO_3$. Supporting this conclusion, characteristic peaks from an In_2O_3 phase was observed in compositions with x≤0.70.

The relative permittivity and tan δ as a function of temperature for the compositions with x=0.95−0.75 are shown in Fig. 3. The temperature at which the relative permittivity

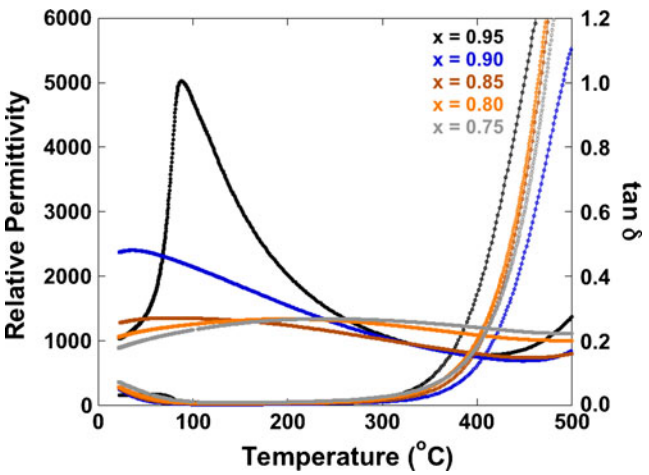

Fig. 3 Temperature dependence of relative permittivity and tan δ of $xBaTiO_3 - (1\text{-}x)(0.5Bi(Zn_{1/2}Ti_{1/2})O_3 - 0.5BiInO_3)$ ceramics measured at 10 kHz, where x=0.95−0.75

Table 1 Temperature at which the relative permittivity is maximum (T_{max}), relative permittivity, and tan δ of $xBaTiO_3 - (1\text{-}x)(0.5Bi(Zn_{1/2}Ti_{1/2})O_3 - 0.5BiInO_3)$ ceramics, where x=0.95−0.75. Data obtained from 10 kHz measurement

Composition (x)	T_{max} (°C)	Relative permittivity at T_{max}	Room temperature	
			Relative permittivity	tan δ
0.95	88	5,030	1,060	0.032
0.90	36	2,400	2,380	0.046
0.85	76	1,350	1,290	0.049
0.80	199	1,340	1,070	0.053
0.75	241	1,340	910	0.068

is maximum (T_{max}) decreased from 126 °C, for pure $BaTiO_3$, to near room temperature as x decreased, for the compositions with x≥0.90. However, for the compositions with x<0.90, when x decreased further, the T_{max} increased. The increase in T_{max} in the pseudocubic phase region was also observed in the $BaTiO_3 - Bi(Zn_{1/2}Ti_{1/2})O_3$ [15], $BaTiO_3 - BiScO_3$ [14], and $BaTiO_3 - Bi(Zn_{1/2}Ti_{1/2})O_3 - BiScO_3$ [22]. It should also be noted that only the composition with x=0.95 exhibited a sharp phase transition. For the composition with 0.75≤x≤0.90, the phase transition became increasingly diffuse with a decrease in the room temperature permittivity. This broad temperature independent maximum is a common characteristic of a weakly coupled relaxor material [14]. Data for T_{max}, relative permittivity, and tan δ for compositions with x=0.95−0.75 are listed in Table 1.

The ferroelectric hysteresis behavior was investigated at room temperature under an applied electric field of 50 kV/cm and a measurement frequency of 1 Hz, as shown in Fig. 4. At x=0.95, normal ferroelectric behavior was observed with a maximum polarization (P_{max}) of 17.3 μC/cm^2, remnant polarization (P_r) of 11.6 μC/cm^2, and coercive field

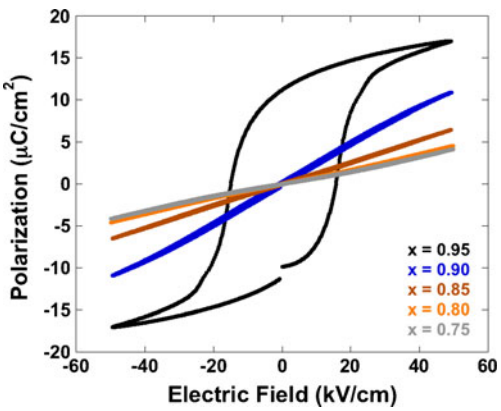

Fig. 4 Room temperature polarization versus electric field hysteresis measured at 10 Hz of $xBaTiO_3 - (1\text{-}x)(0.5Bi(Zn_{1/2}Ti_{1/2})O_3 - 0.5BiInO_3)$ ceramics where x=0.95−0.75

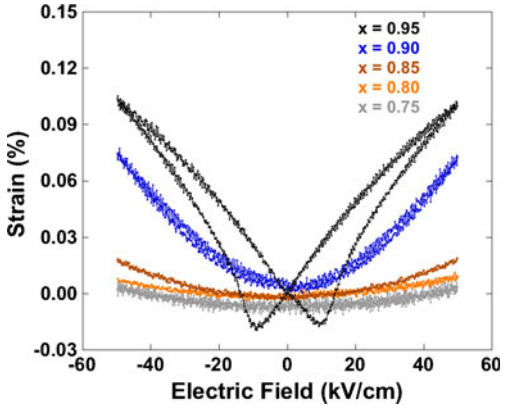

Fig. 5 Room temperature bipolar strain versus electric field measured at 0.1 Hz of $xBaTiO_3 - (1\text{-}x)(0.5Bi(Zn_{1/2}Ti_{1/2})O_3 - 0.5BiInO_3)$ ceramics where x=0.95−0.75

(E_C) of 15.4 kV/cm. At x=0.9, while some minor tetragonal features were seen in the XRD data the hysteresis behavior is largely linear with only a small degree of saturation at the highest applied fields. As the $BaTiO_3$ concentration decreased, there was a precipitous decrease in P_{max} to 4.2 $\mu C/cm^2$ for x=0.75. A loss of hysteretic behavior and a drastic decrease in P_r to nearly zero was observed for compositions with x≤0.90. These compositions exhibited slim loops with negligible hysteresis and a subtle non-linear feature that is similar to that observed in the PLZT system [23].

The electromechanical strain was investigated at room temperature with a measurement frequency of 0.1 Hz and an applied electric field of 50 kV/cm. The bipolar strain versus electric field for the compositions with x=0.95−0.75 are shown in Fig. 5. For the composition with x=0.95, the bipolar strain showed a typical ferroelectric "butterfly" loop, which exhibits a maximum strain of 0.101 %. When the concentration of $BaTiO_3$ decreased further (x=0.90), the butterfly loops disappeared and transformed to parabolic curves with negligible hysteresis. The maximum strain for this composition was 0.071 %. For compositions with x≤ 0.85, in the pseudocubic phase region, the maximum strain drastically decreased to a value of 0.019 % with no hysteresis and further decreased with x. In addition, the high field effective piezoelectric coefficient (d_{33}^*) was also calculated

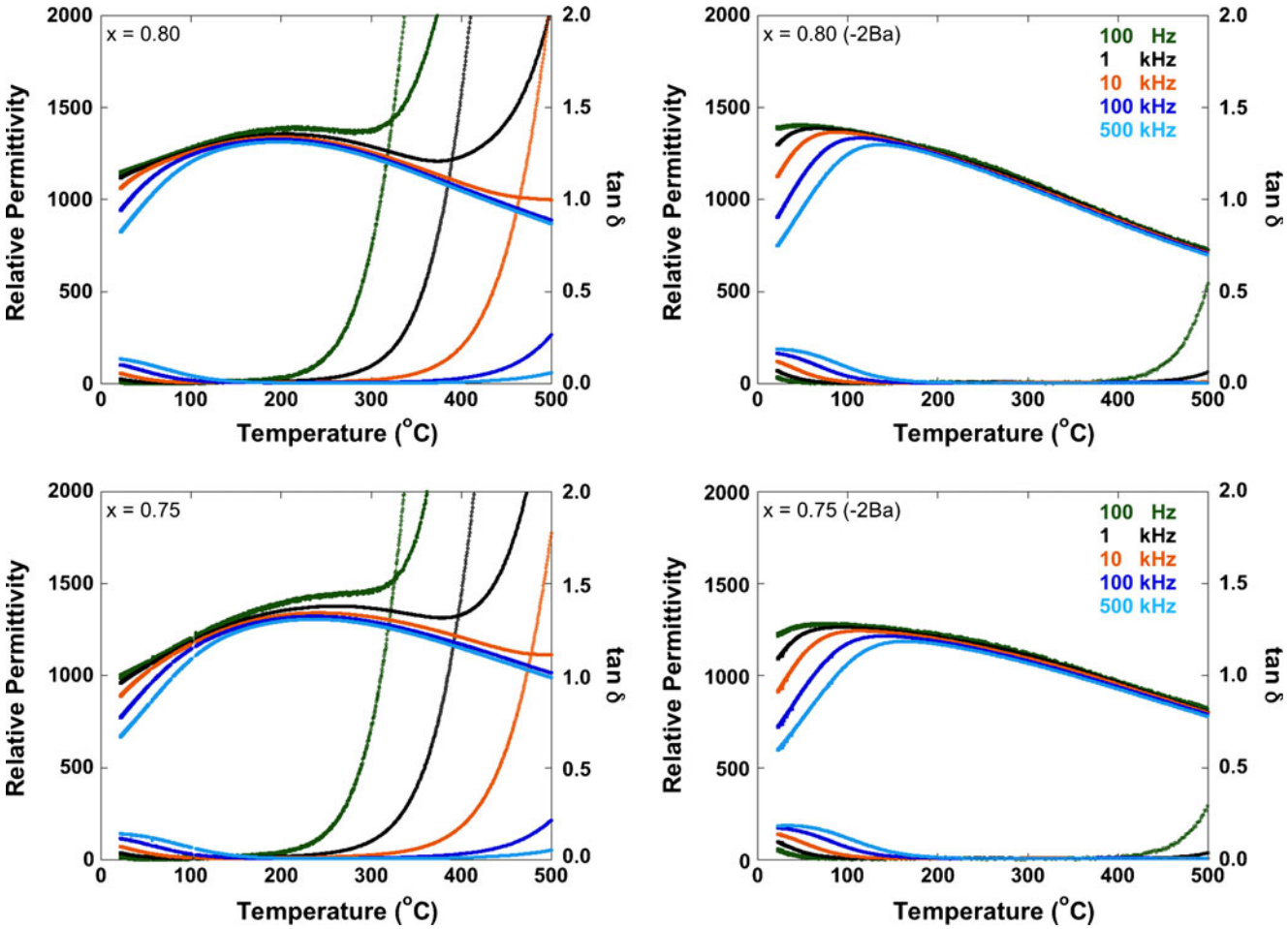

Fig. 6 Relative permittivity and tan δ as a function of temperature of stoichiometric (left) and 2 mol% Ba-deficient (right) $xBaTiO_3 - (1\text{-}x)(0.5Bi(Zn_{1/2}Ti_{1/2})O_3 - 0.5BiInO_3)$ ceramics where x=0.75 and 0.80

Table 2 Temperature at which the relative permittivity is maximum (T_{max}), relative permittivity, and tan δ of stoichiometric and 2 mol% Ba-deficient of $xBaTiO_3 - (1\text{-}x)(0.5Bi(Zn_{1/2}Ti_{1/2})O_3 - 0.5BiInO_3)$ ceramics, where x=0.80 and 0.75. Data obtained from 10 kHz measurement

Composition (x)	T_{max} (°C)	25 °C		400 °C	
		Relative permittivity	tan δ	Relative permittivity	tan δ
0.80	199	1,080	0.052	1,090	0.201
0.80 (−2Ba)	88	1,150	0.114	890	0.007
0.75	241	910	0.068	1,210	0.183
0.75 (−2Ba)	113	930	0.136	950	0.008

from the maximum strain. The d_{33}* of 202 and 142 pm/V were obtained for the compositions with x=0.95 and 0.90, respectively.

For high temperature capacitor applications, a high relative permittivity with minimal temperature dependence is needed and the broad and diffuse transition observed in compositions x=0.75 and 0.80 are well-suited for this purpose. However, the increase in the low frequency dielectric loss, which is indicative of semiconduction, at temperatures exceeding ~200 °C is one of the main concerns for such applications. Therefore, to lower the dielectric loss especially at high temperature, Ba vacancies were introduced to the compositions with x=0.75 and 0.80. Previous studies on $0.8BaTiO_3 - 0.2Bi(Zn_{1/2}Ti_{1/2})O_3$ solid solutions showed a significant decrease in the low frequency dielectric loss at high temperature in compositions containing 2 mol% Ba vacancies [16]. As shown in Fig. 6, the dielectric characteristics of the x=0.75 and 0.80 compositions were similar to that of the BT – BZT binary system. The T_{max} sharpened and shifted to lower temperatures with a relative permittivity of more than 1,000 for the compositions containing Ba vacancies. In addition, a tan δ value of less than 0.05 was observed over the temperature range of 50–490 °C for the both compositions. The measured values for T_{max}, relative permittivity and tan δ at 25 and 400 °C are listed in Table 2.

It should be noted that the introduction of Ba vacancies into the ternary compounds affected not only the high temperature dielectric properties but also the polarization hysteresis as shown in Fig. 7. The weak non-linear characteristic observed in the stoichiometric compositions, denoted as S in the figure, disappeared when the Ba vacancies, denoted as -2Ba, were introduced.

The DC resistivity measurements were conducted at different temperatures from room temperature up to 500 °C. Only the Ba-deficient compositions (−2Ba) with x=0.75 and 0.80 were investigated, as previous work has shown that significantly higher high temperature resistivities can be obtained in Ba-deficient compositions [16, 17]. As shown in Fig. 8, the resistivity of 149±2 GΩ.cm was observed over the temperature range of 25–225 °C for the composition x=0.75. A lower resistivity of 139±2 GΩ.cm for the composition with x=0.80 was observed over the same temperature range. A sharp decrease in resistivity was observed at temperatures higher than 275 °C. The activation energy (E_A) of conduction was also calculated be using an Arrhenius equation. Large values of E_A of 1.85 and 1.69 eV were observed for the compositions with x=0.75 and 0.80, respectively. These large activation energies are comparable to the activation energies measured for BT-BZT (E_A=1.7 eV) and BT-BZT-$BiScO_3$ (E_A=1.4 eV).

The optical band gap energies of these compounds was estimated from a diffuse reflectance measurement. By using the Kubelka-Munk and Tauc equations, optical (indirect) band gap values of 3.26 and 3.22 eV were observed for the x=0.75 and 0.80 compositions, respectively. These values showed similar trend as of the activation energy obtained from resistivity measurement, i.e., the composition with x=0.75 exhibited larger E_A and wider E_g than that of x=0.80. Thus, these results confirmed that compositions with smaller x, that is a larger BZT-BI content, maintained a higher resistivity to high temperatures.

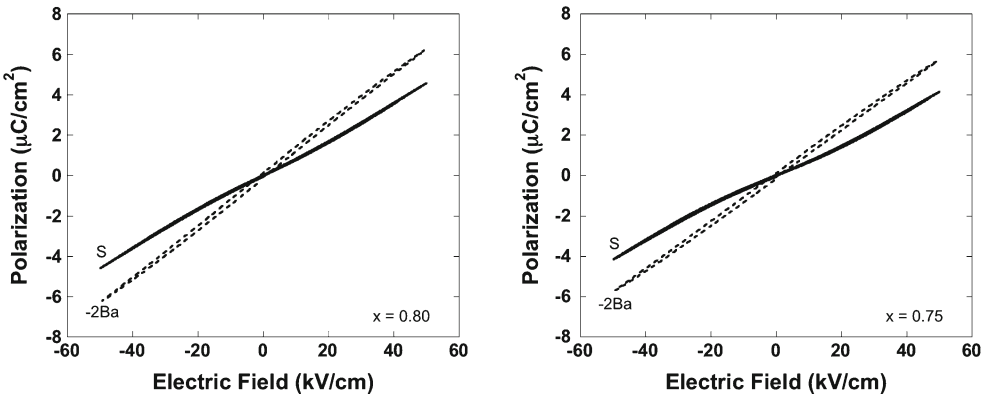

Fig. 7 Room temperature polarization versus electric field hysteresis measured at 10 Hz of stoichiometric (S) and 2 mol% Ba-deficient (−2Ba) of $xBaTiO_3 - (1\text{-}x)(0.5Bi(Zn_{1/2}Ti_{1/2})O_3 - 0.5BiInO_3)$ ceramics, where x=0.80 and 0.75

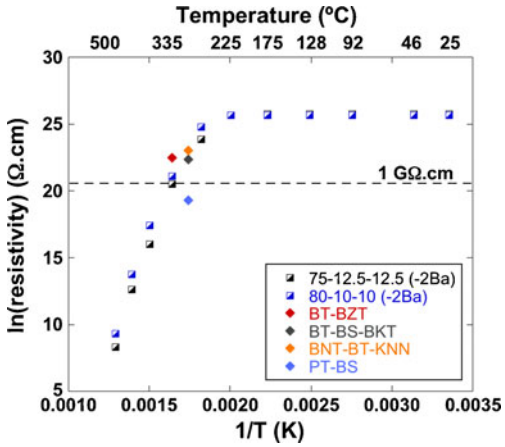

Fig. 8 Temperature dependence of DC resistivity of the 2 mol% Ba-deficient (−2Ba) of $xBaTiO_3 - (1\text{-}x)(0.5Bi(Zn_{1/2}Ti_{1/2})O_3 - 0.5BiInO_3)$ ceramics, where x=0.80 and 0.75, and 0.8BT-0.2BZT [16], 0.8(0.6BT-0.4BS)-0.2BKT [24], 0.82(0.94BNT-0.06BT)-0.18KNN [19], 0.64PT-0.36BS [25]

The resistivity of related materials from literature [16, 24, 25] are also included in Fig. 8. The resistivity values of more than 1 GΩ.cm for the BT-BZT-BI (x=0.75 and 0.80) in this work were comparable to published work on the ternary systems BT-BS-BKT [24] and BNT-BT-KNN [19] at 300 °C and higher than that of PT-BS [25]. However, the resistivity of the binary BT-BZT [16] compound at 335 °C is superior to that of the ternary system BT-BZT-BI.

The temperature dependence of the RC time constant was observed for the compositions with x=0.75 and 0.80, as shown in Fig. 9. A similar trend of temperature dependence of the RC time constant and the resistivity was observed. For x=0.75 and 0.80, the RC time constant of 16±1 s was observed over the temperature range of 25–225 °C. At higher temperatures, it decreased to a value close to 10^{-7} s at 500 °C. It was found to be comparable to the related

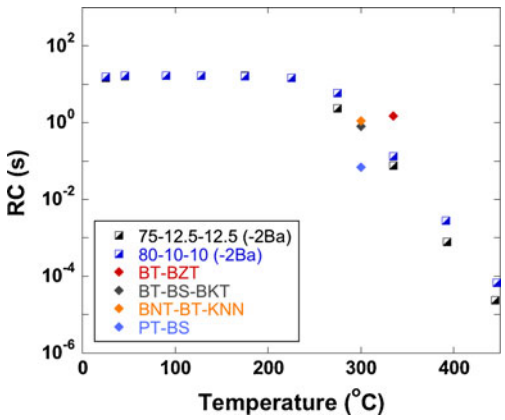

Fig. 9 Temperature dependence of RC time constant of the 2 mol% Ba-deficient (−2Ba) of $xBaTiO_3 - (1\text{-}x)(0.5Bi(Zn_{1/2}Ti_{1/2})O_3 - 0.5BiInO_3)$ ceramics, where x=0.80 and 0.75, and 0.8BT-0.2BZT [16], 0.8(0.6BT-0.4BS)-0.2BKT [24], 0.82(0.94BNT-0.06BT)-0.18KNN [19], 0.64PT-0.36BS [25]

materials at 300 °C, see Fig. 9. As with the resistivity data, at 335 °C, the binary BT-BZT compound exhibited a larger RC time constant (1.47 s) than that of the ternary BT-BZT-BI samples (0.13 s for x=0.75 and 0.076 s for x=0.80).

The temperature coefficient of the relative permittivity at 300 °C (TCε) was calculated from the dielectric data over the temperature range of 200–400 °C at 1 kHz using the following expression;

$$TC\varepsilon = (1/\varepsilon_{300})(-(\varepsilon_{200} - \varepsilon_{400})/200)$$

As shown in Table 3, for the compositions containing 2 mol% Ba vacancies, a negative value of TCε were obtained.

This result showed that the introduction of $BiInO_3$ enhanced the temperature stability of the dielectric properties, with TCε values approaching −1,000 ppm/K for the x=0.80 composition. At higher concentrations of BZT-BI (x=0.75), TCε increased to a value closer to zero. This suggests that temperature independent dielectric properties could be obtained by increasing the BZT-BI content. However, due to the solubility limit of the ternary compound, compositions with x<0.75 could not be obtained with single phase perovskite, which would have the effect of diluting the relative permittivity. Additional ternary compositions in the BT-BZT-BI system are being investigated in order find a perovskite phase with a high relative permittivity and truly temperature independent properties.

Following the theoretical framework of Harrop [26] due to the effects of thermal expansion and permittivity ($-\alpha_l\varepsilon_r$) it is unusual to find a material with such a large permittivity and temperature stable properties. The BT-BZT-BI material in this paper is unique in that it deviates from this trend. The anomalous properties of this material are closely linked to the diffuse phase transition, which effectively broadens the dielectric maximum over a wide temperature range.

4 Conclusions

Solid solutions of $xBaTiO_3 - (1\text{-}x)(0.5Bi(Zn_{1/2}Ti_{1/2})O_3 - 0.5BiInO_3)$, where x=0.95−0.60, were investigated for high

Table 3 Temperature coefficient of the relative permittivity at 300 °C (TCε) of the 2 mol% Ba-deficient of $xBaTiO_3 - (1\text{-}x)(0.5Bi(Zn_{1/2}Ti_{1/2})O_3 - 0.5BiInO_3)$ ceramics, where x=0.80 and 0.75, and the $0.8BaTiO_3 - 0.2Bi(Zn_{1/2}Ti_{1/2})O_3$ ceramics. Data obtained from 1 kHz measurement in the temperature range of 200–400 °C

Composition (x)	TCε (ppm/°C)	Reference
0.8BT-0.2BZT	−2261	[16]
0.8BT-0.1BZT-0.1BI	−1644	this work
0.75BT-0.125BZT-0.125BI	−1114	this work

temperature capacitor applications. At compositions with $x \geq 0.75$, the compounds formed a single-phase perovskite exhibiting a phase transformation from tetragonal to pseudocubic symmetry as observed from x-ray diffraction patterns as x decreased from 0.95 to 0.75. The tetragonality and the temperature at which the relative permittivity is maximum (T_{max}), in tetragonal phase region, $x \geq 0.90$, decreased when the $Bi(Zn_{1/2}Ti_{1/2})O_3 - BiInO_3$ content increased. In the pseudocubic phase region, $x < 0.90$, the lattice parameter and T_{max} increased when x decreased. Additionally, in the pseudocubic phase region a highly broad and diffuse phase transition was observed along with a linear dielectric response. By introducing 2 mol% of Ba vacancies to the composition with $x = 0.80$, low dielectric loss values ($\tan \delta < 0.05$) persisted over the temperature range of 30–490 °C. This coincided with high resistivity values that exhibited an activation energy of ~1.8 eV at high temperatures, suggesting an intrinsic conduction mechanism. It also improved the temperature stability of the dielectric properties, whereby TCε decreased from −2261 ppm/°C, for the binary 0.8BT-0.2BZT, to −1644 ppm/°C, for the ternary compound ($x = 0.80$).

References

1. G.H. Haertling, J. Am. Ceram. Soc. **82**, 797 (1999)
2. R.E. Eitel, C.A. Randall, T.R. Shrout, P.W. Rehrig, W. Hackenberger, S.E. Park, Jpn. J. Appl. Phys., Part 1 **40**, 5999 (2001)
3. I. Grinberg, M.R. Suchomel, P.K. Davies, A.M. Rappe, J. Appl. Phys. **98**, 094111 (2005)
4. M.R. Suchomel, P.K. Davies, J. Appl. Phys. **96**, 1489 (2004)
5. M.R. Suchomel, P.K. Davies, Appl. Phys. Lett. **86**, 262905 (2005)
6. I. Grinberg, M.R. Suchomel, W. Dmowski, S. E. Mason., H. Wu, P. K. Davies, and A. M. Rappe. Phys. Rev. Lett. **98**, 107601 (2007)
7. J. Chen, X. Tan, W. Jo, J. Rodel, J. Appl. Phys. **106**, 034109 (2009)
8. C.A. Randall, R. Eitel, B. Jones, T.R. Shrout, D.I. Woodward, I.R. Reaney, J. Appl. Phys. **95**, 3633 (2004)
9. S.M. Choi, C.J. Stringer, T.R. Shrout, C.A. Randall, J. Appl. Phys. **95**, 034108 (2005)
10. R.E. Eitel, C.A. Randall, T.R. Shrout, S.E. Park, Jpn. J. Appl. Phys., Part 1 **41**, 1999 (2002)
11. A. Sehirlioglu, A. Sayir, F. Dynys, J. Appl. Phys. **106**, 014102 (2009)
12. R. Duan, R.F. Speyer, E. Alberta, T.R. Shrout, J. Mater. Res. **19**, 2185 (2004)
13. S. Zhang, R. Xia, C.A. Randall, T.R. Shrout, R. Duan, R.F. Speyer, J. Mater. Res. **20**, 2067 (2005)
14. H. Ogihara, C.A. Randall, S. Trolier-McKinstry, J. Am. Ceram. Soc. **92**, 110 (2009)
15. C.-C. Huang, D.P. Cann, J. Appl. Phys. **104**, 024117 (2008)
16. N. Raengthon, D.P. Cann, IEEE Trans. Ultrason. Ferroelectr. Freq. Control **58**, 1954 (2011)
17. N. Raengthon, D.P. Cann, J. Am. Ceram. Soc.. doi:10.1111/j.1551-2916.2011.05018.x
18. K. Datta, E. Suard, P.A. Thomas, Appl. Phys. Lett. **96**, 221902 (2010)
19. R. Dittmer, W. Jo, D. Damjanovic, J. Rodel, J. Appl. Phys. **109**, 034107 (2011)
20. P. Jarupoom, E. Patterson, B. Gibbons, G. Rujijanagul, R. Yimnirun, D. Cann, Appl. Phys. Lett. **99**, 152901 (2011)
21. J.B. Lim, S. Zhang, N. Kim, T.R. Shrout, J. Am. Ceram. Soc. **92**, 679 (2009)
22. C.-C. Huang, D.P. Cann, X. Tan, N. Vittayakorn, J. Appl. Phys. **102**, 044103 (2007)
23. D. Viehland, D. Forst, Z. Xu, J.-F. Li, J. Am. Ceram. Soc. **78**, 2101 (1995)
24. J.B. Lim, S. Zhang, N. Kim, T.R. Shrout, J. Am. Ceram. Soc. **93**, 679 (2009)
25. S. Zhang, E.F. Alberta, R.E. Eitel, C.A. Randall, T.R. Shrout, IEEE Trans. Ultrason. Ferroelectr. Freq. Control **52**, 2131 (2005)
26. P.J. Harrop, J. Mater. Sci. **4**, 370 (1969)